

Traja: A Python toolbox for animal trajectory analysis

Justin Shenk^{1, 2}, Wolf Byttner³, Saranraj Nambusubramaniyan¹, and Alexander Zoeller⁴

¹ VisioLab, Berlin, Germany ² Radboud University, Nijmegen, Netherlands ³ Rapid Health, London, England, United Kingdom ⁴ Independent researcher

DOI: [10.21105/joss.00118](https://doi.org/10.21105/joss.00118)

Software

- [Review](#) ↗
- [Repository](#) ↗
- [Archive](#) ↗

Editor: [Arfon Smith](#) ↗

Reviewers:

- [@arfon](#)

Submitted: 04 November 2016

Published: 05 December 2016

License

Authors of papers retain copyright and release the work under a Creative Commons Attribution 4.0 International License ([CC BY 4.0](#)).

Summary

There are generally four categories of trajectory data: mobility of people, mobility of transportation vehicles, mobility of animals, and mobility of natural phenomena (Zheng, 2015). Animal tracking is important for fields as diverse as ethology, optimal foraging theory, and neuroscience. Mouse behavior, for example, is a widely studied in biomedical and brain research in models of neurological disease such as stroke.¹

Several tools exist which allow analyzing mouse locomotion. Tools such as Ethovision (Spink et al., 2001) and DeepLabCut (Mathis et al., 2018) allow converting video data to pose coordinates, which can further be analyzed by other open source tools. DLCAnalyzer² provides a collection of R scripts for analyzing positional data, in particular visualizing, classifying and plotting movement. B-SOiD (Hsu & Yttri, 2020) allows unsupervised clustering of behaviors, extracted from the pose coordinate outputs of DeepLabCut. SimBA (sgoldenlab et al., 2021) provides several classifiers and tools for behavioral analysis in video streams in a Windows-based graphical user interface (GUI) application.

These tools are primarily useful for video data, which is not available for the majority of animal studies. For example, video monitoring of home cage mouse data is impractical today due to housing space constraints. Researchers using Python working with non-visual animal tracking data sources are not able to fully leverage these tools. Thus, a tool that supports modeling in the language of state-of-the-art predictive models (Amirian et al., 2019; Chandra et al., 2019; Liang et al., 2019), and which provides animal researchers with a high-level API for multivariate time series feature extraction, modeling and visualization is needed.

Traja is a Python package for statistical analysis and computational modelling of trajectories. Traja extends the familiar pandas (McKinney, 2010; team, 2020) methods by providing a pandas accessor to the `df.traja` namespace upon import. The API for Traja was designed to provide an object-oriented and user-friendly interface to common methods in analysis and visualization of animal trajectories. Traja also interfaces well with relevant spatial analysis packages in R (e.g., `trajr` (McLean & Volponi, 2018) and `adehabitat` (Calenge, 2006)), Shapely (Gillies & others, 2007–), and MovingPandas (Graser, 2019) allowing rapid prototyping and comparison of relevant methods in Python. A comprehensive source of documentation is provided on the home page (<http://traja.readthedocs.io>).

Statement of Need

The data used in this project includes animal trajectory data provided by <http://www.tecniplast.it>, manufacturer of laboratory animal equipment based in Varese, Italy, and Radboud University,

¹The examples in this paper focus on animal motion, however it is useful for other domains.

²<https://github.com/ETHZ-INS/DLCAnalyzer>

Nijmegen, Netherlands. Tecniplast provided the mouse locomotion data collected with their Digital Ventilated Cages (DVC). The extracted coordinates of the mice requires further analysis with external tools. Due to lack of access to equipment, mouse home cage data is rather difficult to collect and analyze, thus few studies have been done on home cage data. Furthermore, researchers who are interested in developing novel algorithms must implement from scratch much of the computational and algorithmic infrastructure for analysis and visualization. By packaging a library that is particularly useful for animal locomotion analysis, future researchers can benefit from access to a high-level interface and clearly documented methods for their work.

Other toolkits for animal behavioral analysis either rely on visual data (Mathis et al., 2018; Sridhar, 2017) to estimate the pose of animals or are limited to the R programming language (McLean & Volponi, 2018). Prototyping analytical approaches and exploratory data analysis is furthered by access to a wide range of methods which existing libraries do not provide. Python is the *de facto* language for machine learning and data science programming, thus a toolkit in Python which provides methods for prototyping multivariate time series data analysis and deep neural network modeling is needed.

Overview of the Library

Traja targets Python because of its popularity with data scientists. The library leverages the powerful pandas library (McKinney, 2010), while adding methods specifically for trajectory analysis. When importing Traja, the Traja namespace registers itself within the pandas dataframe namespace via `df.traja`.

The software is structured into three parts. These provide functionality to transform, analyse and visualize trajectories. Full details are available at <https://traja.readthedocs.io/>. The trajectory module provides analytical and preprocessing functionalities. The `models` subpackage provides both traditional and neural network-based tools to determine trajectory properties. The `plotting` module allows visualizing trajectories in various ways.

Data, e.g., x and y coordinates, are stored as one-dimensional labelled arrays as instances of the pandas native `Series` class. Further, subclassing the pandas `DataFrame` allows providing an API that mirrors the pandas API which is familiar to most data scientists, thus reducing the barrier for entry while providing methods and properties specific to trajectories for rapid prototyping. Traja depends on Matplotlib (Hunter, 2007) and Seaborn (Waskom, 2021) for plotting and NumPy (Harris et al., 2020) for computation.

Trajectory Data Sources

Trajectory data as time series can be extracted from a wide range of sources, including video processing tools as described above, GPS sensors for large animals or via home cage floor sensors, as described in the section below. The methods presented here are implemented for orthogonal coordinates (x , y) primarily to track animal centroids, however with some modification they could be extended to work in 3-dimensions and with body part locations as inputs. Traja is thus positioned at the end of the data scientist's chain of tools with the hope of supporting prototyping novel data processing approaches. A sample dataset of jaguar movement (Morato et al., 2018) is provided in the `traja.dataset` subpackage.

Mouse Locomotion Data

The data samples presented here³ are in 2-dimensional location coordinates, reflecting the mouse home cage (25x12.5 cm) dimensions. Analytical methods relevant to 2D rectilinear

³This dataset has been collected for other studies of our laboratory (Shenk et al., 2020).

83 analysis of highly constrained spatial coordinates are thus primarily considered.

84 High volume data like animal trajectories has an increased tendency to have missing data
85 due to data collection issues or noise. Filling in the missing data values, referred to as
86 *data imputation*, is achieved with a wide variety of statistical or learning-based methods. As
87 previously observed, data science projects typically require at least 95% of the time to be spent
88 on cleaning, pre-processing and managing the data (Bosch et al., 2021). Therefore, several
89 methods relevant to preprocessing animal data are demonstrated throughout the following
90 sections.

91 Spatial Trajectory

92 A *spatial trajectory* is a trace generated by a moving object in geographical space. Trajectories
93 are traditionally modelled as a sequence of spatial points like:

$$T_k = \{P_{k1}, P_{k2}, \dots\}$$

94 where $P_{ki} (i \geq 1)$ is a point in the trajectory.

95 Generating spatial trajectory data via a random walk is possible by sampling from a distribution
96 of angles and step sizes (Kareiva & Shigesada, 1983; McLean & Volponi, 2018). A correlated
97 random walk (Figure 1) is generated with `traja.generate`.

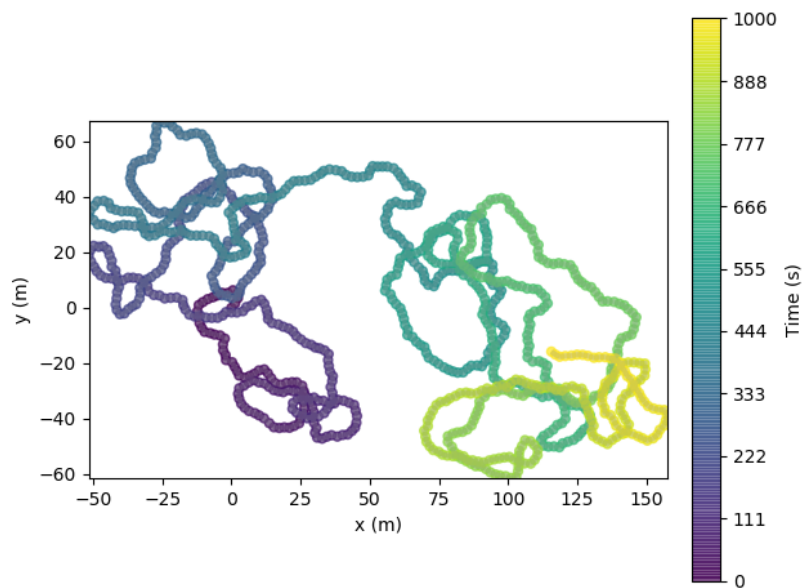


Figure 1: Generation of a random walk

98 Spatial Transformations

99 Transformation of trajectories can be useful for comparing trajectories from various geospatial
100 coordinates, data compression, or simply for visualization purposes.

101 Feature Scaling

102 Feature scaling is common practice for preprocessing data for machine learning (Grus, 2015)
103 and is essential for even application of methods to attributes. For example, a high dimensional

feature vector $\mathbf{x} \in \mathbb{R}^n$ where some attributes are in $(0, 100)$ and others are in $(-1, 1)$ would lead to biases in the treatment of certain attributes. To limit the dynamic range for multiple data instances simultaneously, scaling is applied to a feature matrix $X = \{\mathbf{x}_1, \mathbf{x}_2, \dots, \mathbf{x}_N\} \in \mathbb{R}^{n \times N}$, where n is the number of instances.

Min-Max Scaling To guarantee that the algorithm applies equally to all attributes, the normalized feature matrix \hat{X} is rescaled into range $(0, 1)$ such that

$$\hat{X} = \frac{X - X_{min}}{X_{max} - X_{min}}.$$

Standardization The result of standardization is that the features will be rescaled to have the property of a standard normal distribution with $\mu = 0$ and $\sigma = 1$ where μ is the mean (average) of the data and σ is the standard deviation from the mean. Standard scores (also known as **z-scores** are calculated such that

$$z = \frac{x - \mu}{\sigma}.$$

Scaling Scaling a trajectory is implemented for factor f in scale where $f \in \mathbb{R} : f \in (-\infty, +\infty)$.

Rotation

Rotation of a 2D rectilinear trajectory is a coordinate transformation of orthonormal bases x and y at angle θ (in radians) around the origin defined by

$$\begin{bmatrix} x' \\ y' \end{bmatrix} = \begin{bmatrix} \cos\theta & \sin\theta \\ -\sin\theta & \cos\theta \end{bmatrix} \begin{bmatrix} x \\ y \end{bmatrix}$$

with angle θ where $\theta \in \mathbb{R} : \theta \in [-180, 180]$.

Trip Grid

One strategy for compressing the representation of trajectories is binning the coordinates to produce an image as shown in Figure 2.

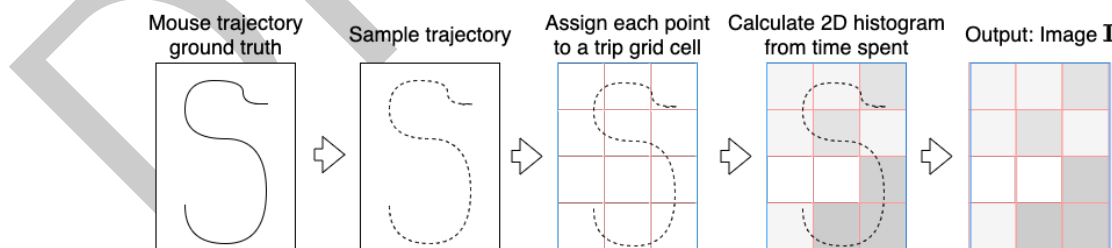


Figure 2: Trip grid image generation from mouse trajectory.

Allowing computation on discrete variables rather than continuous ones has several advantages stemming from the ability to store trajectories in a more memory efficient form.⁴ The advantage is that computation is generally faster, more data can fit in memory in the case of complex models, and item noise can be reduced.

Creation of an $M \times N$ grid allows mapping trajectory T_k onto uniform grid cells. Generalizing the nomenclature of (Wang, 2017) to rectangular grids, C_{mn} ($1 \leq m \leq M; 1 \leq n \leq N$) denotes the cell in row m and column n of the grid. Each point P_{ki} is assigned to a cell

⁴In this experiment, for example, data can be reduced from single-precision floating point (32 bits) to 8-bit unsigned integer (*uint8*) format.

132 $C(m, n)$. The result is a two-dimensional image $M * N$ image I_k , where the value of pixel
133 $I_k(m, n)$ ($1 \leq m, n \leq M$) indicates the relative number of points assigned to cell C_{mn} .
134 Partitioning of spatial position into separate grid cells is often followed by generation of
135 hidden Markov models (Jeung et al., 2007) (see below) or visualization of heat maps (Figure
136 3).

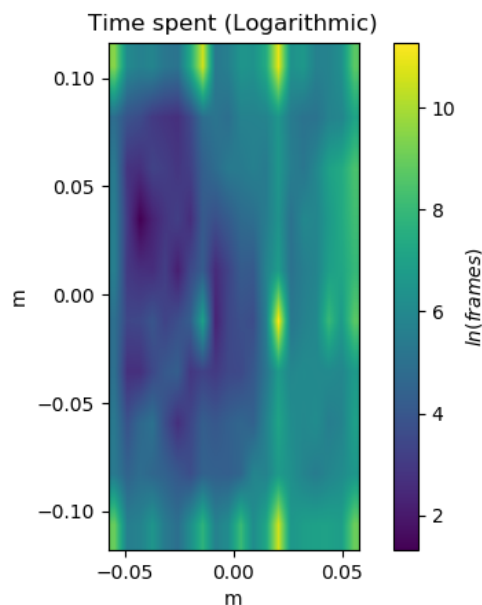


Figure 3: Visualization of heat map from bins generated with `df.trip_grid`. Note regularly spaced artifacts (bright yellow) in this sample due to a bias in the sensor data interpolation. This type of noise can be minimized by thresholding or using a logarithmic scale, as shown above.

137 Smoothing

138 Smoothing a trajectory can also be achieved with Traja using Savitzky-Golay filtering with
139 `smooth_sg` (Savitzky & Golay, 1964).

140 Resampling and Rediscretizing

141 Trajectories can be resampled by time or rediscretized by an arbitrary step length. This can
142 be useful for aligning trajectories from various data sources and sampling rates or reducing
143 the number of data points to improve computational efficiency. Care must be taken to select
144 a time interval which maintains information on the significant behavior. If the minimal time
145 interval observed is selected for the points, calculations will be computationally intractable for
146 some systems. If too large of an interval is selected, we will fail to capture changes relevant
147 to the target behavior in the data.

148 Resampling by time is performed with `resample_time` (Figure 4). Rediscretizing by step
149 length is performed with `rediscretize`.

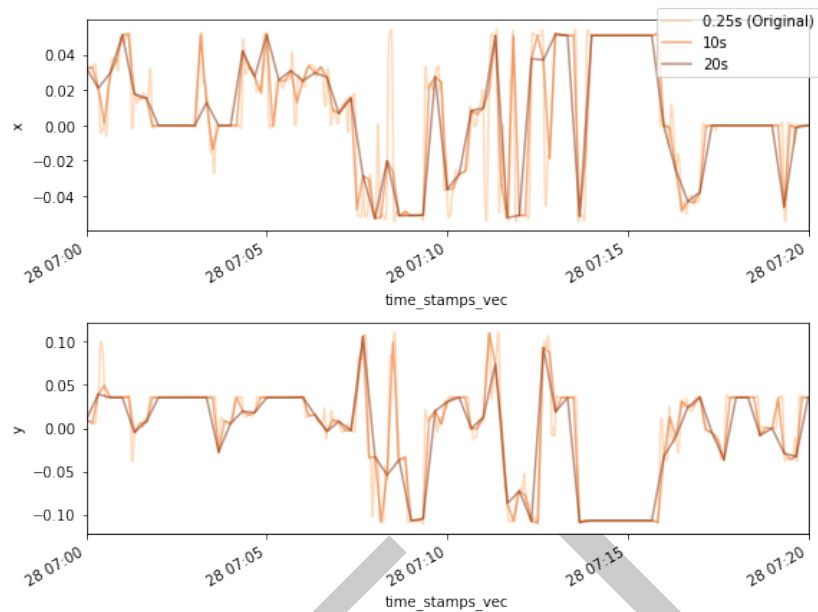


Figure 4: Resampling trajectories by different time scales is performed with `resample_time`.

For example, the Fortasyn dataset (Shenk et al., 2020) demonstrated in this paper was sampled at 4 Hz and converted to single-precision floating point data. Pandas dataframes store this data in 4 bytes, thus there are approximately 4.15 MB⁵ bytes required to store data for x and y dimensions plus an index reference for a single day. In the case of (Shenk et al., 2020), 24 mice were observed over 35 days. This translates to 3.4 GB (10⁹) of storage capacity for the uncompressed datasets prior to feature engineering. Thus resampling can be a useful way to reduce the memory footprint for memory constrained processes that have to fit into a standard laptop with 8 GB memory space. A demonstration of how reduction in precision for trajectory data analysis is provided in Figure 4, as applied to a sample from the Fortasyn experiment (Shenk et al., 2020). Broad effects such as cage crossings, for example, can still be identified while downsampling data to a lower frequency, such as 0.1 Hz, reducing the memory footprint by a factor of 40 (4 Hz/0.1 Hz) and providing significant speedups for processing.

Movement Analysis

Traja includes traditional as well as advanced methods for trajectory analysis.

Distance traveled

Distance traveled is a common metric in animal studies - it accounts for the total distance covered by the animal within a given time interval. The distance traveled is typically quantified by summing the square straight-line displacement between discretely sampled trajectories (Rowcliffe et al., 2012; Solla et al., 1999). Alternative distance metrics for the case of animal tracking are discussed in (Noonan et al., 2019).

Let $p(t) = [p_x(t), p_y(t)]$ be a 2×1 vector of coordinates on the ground representing the position of the animal at time t . Then, the distance traveled within the time interval t_1 and t_2 can be computed as a sum of step-wise Euclidean distances

$$p(t_1, t_2) = \sum_{t=t_1+1}^{t_2} d(t),$$

⁵4 × 4 Hz × 60 seconds × 60 minutes × 24 hours × 3 features (x, y, and time)

173 where

$$d(t) = \sqrt{(p_x(t) - p_x(t-1))^2 + (p_y(t) - p_y(t-1))^2}$$

174 is the Euclidean distance between two positions in adjacent time samples.

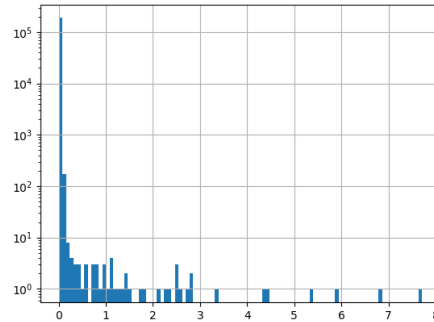


Figure 5: Velocity histogram from one day of mouse activity.

175 Speed

176 Speed or velocity is the first derivative of centroids with respect to time. Peak velocity in a
177 home cage environment is perhaps less interesting than a distribution of velocity observations,
178 as in Figure 5. Additionally, noise can be eliminated from velocity calculations by using a
179 minimal distance moved threshold, as demonstrated in (Shenk et al., 2020). This allows
180 identifying broad-scale behaviors such as cage crossings.

181 Turn Angles

182 Turn angles are the angle between the movement vectors of two consecutive samples. They
183 can be calculated with `calc_turn_angles`.

184 Laterality

185 Laterality is the preference for left or right turning and a *laterality index* is defined as:

$$LI = \frac{RT}{LT + RT}$$

186 where RT is the number of right turns observed and LT is the number of left turns observed.
187 Turns are counted within a left turn angle $\in (\theta, 90)$ and right turn angle $\in (-\theta, -90)$. A
188 turn is considered to have a minimal step length.

189 Periodicity

190 Periodic behaviors are a consequence of the circadian rhythm as well as observing expression
191 of underlying cognitive traits. Some basic implementations of periodic analysis of mouse cage
192 data are presented.

193 Autocorrelation

194 Autocorrelation is the correlation of a signal with a delayed copy of itself as a function of the
195 decay. Basically, it is similarity of observations as a function of the time lag between them.
196 An example is shown in Figure 6.

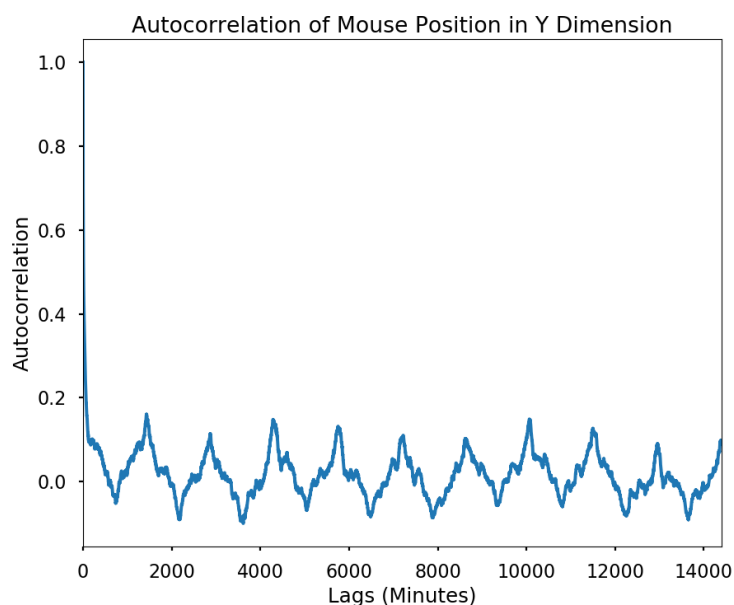


Figure 6: Autocorrelation of the y-dimension reveals daily (1440 minutes) periodic behavior

197 Power Spectrum

198 Power spectrum of a time series signal can be estimated (Figure 7). This is useful for analyzing
199 signals, for example, the influence of neuromotor noise on delays in hand movement (Van Galen
200 et al., 1990).

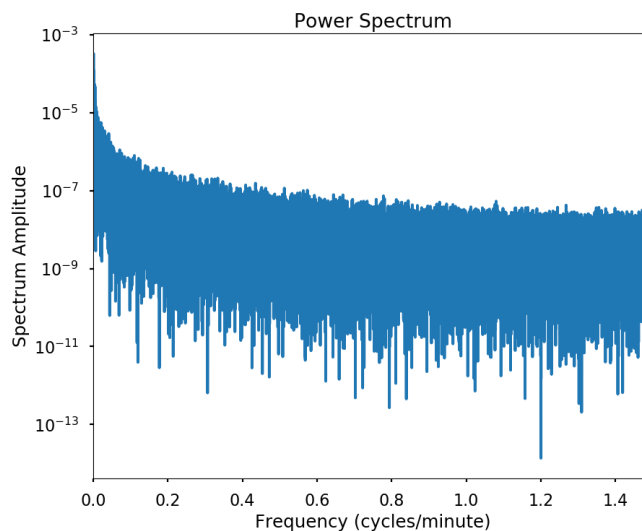


Figure 7: Power Spectral Density. One day of activity reveals fairly smooth power spectral density.

201 Algorithms and Statistical Models

202 Machine Learning for Time Series Data

203 Machine learning methods enable researchers to solve tasks computationally without explicit
204 instructions by detecting patterns or relying on inference. Thus they are particularly relevant
205 for data exploration of high volume datasets such as spatial trajectories and other multivariate
206 time series.

207 Principal Component Analysis

208 Principal Component Analysis projects the data into a linear subspace with a minimum loss
209 of information by multiplying the data by the eigenvectors of the covariance matrix.

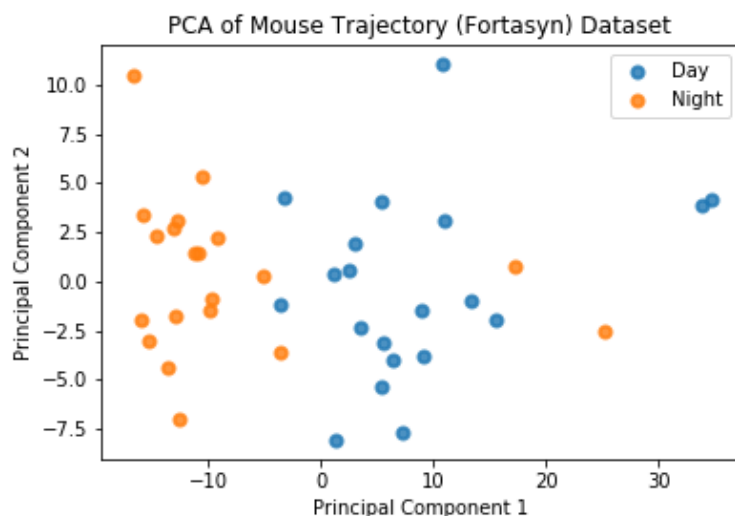


Figure 8: PCA of Fortasyn trajectory data. Daily trajectories (day and night) were binned into 8x8 grids before applying PCA.

210 This requires converting the trajectory to a trip grid (see Figure [2(#fig:tripgridalgo)]{reference-
211 type="ref" reference="fig:tripgridalgo"})) and performing PCA on the grid in 2D (Figure 8)
212 or 3D (Figure 9). Structure in the data is visible if light and dark time periods are compared.

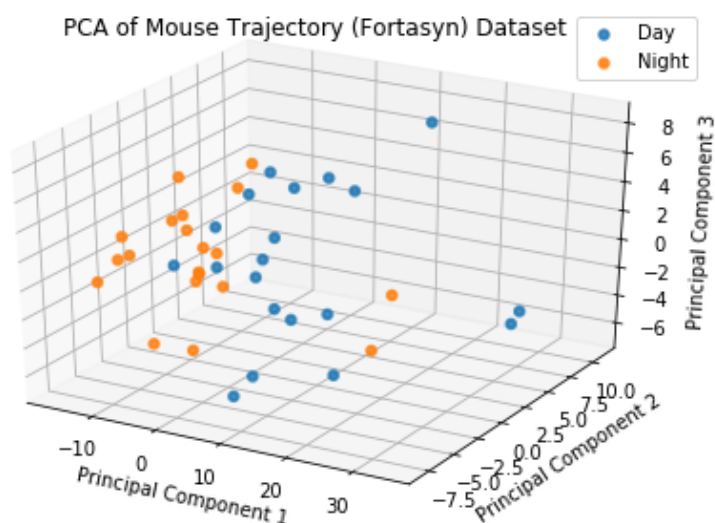


Figure 9: 3D PCA of Fortasyn trajectory data. Daily trajectories (day and night) were binned into 8x8 grids before applying PCA.

213 Clustering

214 Clustering of trajectories is an extensive topic with applications in geospatial data, vehicle and
215 pedestrian classification, as well as molecular identification. K-means clustering is an iterative
216 unsupervised learning method that assigns a label to data points based on a distance function
217 (Bishop, 2006) (Figure 10).

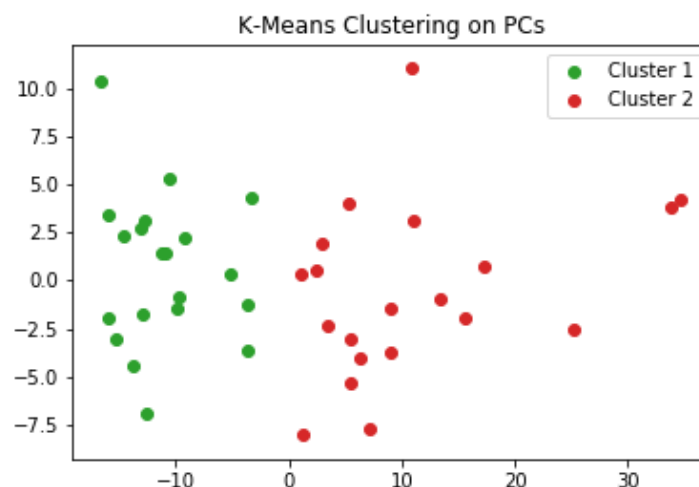


Figure 10: K-means clustering on the results of the PCA shown above reveals a high accuracy of classification, with a few errors. Cluster labels are generated by the model.

218 Hierarchical Agglomerative Clustering

219 Clustering spatial trajectories has broad applications for behavioral research, including unsu-
220 pervised phenotyping (Huang et al., 2020). For mice, hierarchical agglomerative clustering
221 can also be used to identify similarities between groups, for example periodic activity and
222 location visit frequency (Bak et al., 2009).

223 Gaussian Processes

224 Gaussian Processes is a non-parametric method which can be used to model spatial trajectories.
225 This method is not currently implemented in Traja and is thus outside the scope of the current
226 paper, however the interested reader is directed to the excellent text on Gaussian processes by
227 Rasmussen and Williams (Rasmussen & Williams, 2006) for a complete reference and (Cox
228 et al., 2012) for an application to spatial trajectories.

229 Other Methods

230 Fractal Methods

231 Fractal (i.e. multiscale) methods are useful for analyzing transitions and clustering in trajec-
232 tories. For example, search trajectories such as eye movement, hand-eye coordination, and
233 foraging can be analyzed by quantifying the spatial distribution or nesting of temporal point
234 processes using spatial Allen Factor analysis (Huetten et al., 2013; Kerster et al., 2016).

235 Recurrence plots and derivative recurrence factor analysis can be applied to trajectories to
236 identify multiscale temporal processes to study transition or nonlinear parameters in a system,
237 such as postural fluctuation (Ross et al., 2016) and synchrony (Shockley et al., 2003) in
238 humans and to movement of animals such as ants (Neves et al., 2017) and bees (Ayers et al.,
239 2015). These methods are not yet implemented in Traja, but are planned for a future release.

240 Graph Models

241 A graph is a pair $G = (V, E)$ comprising a set of vertices and a set of connecting edges. A
242 probabilistic graphical model of a spatial occupancy grid can be used to identify probabilities
243 of state transitions between nodes. A basic example is given with hidden Markov models
244 below.

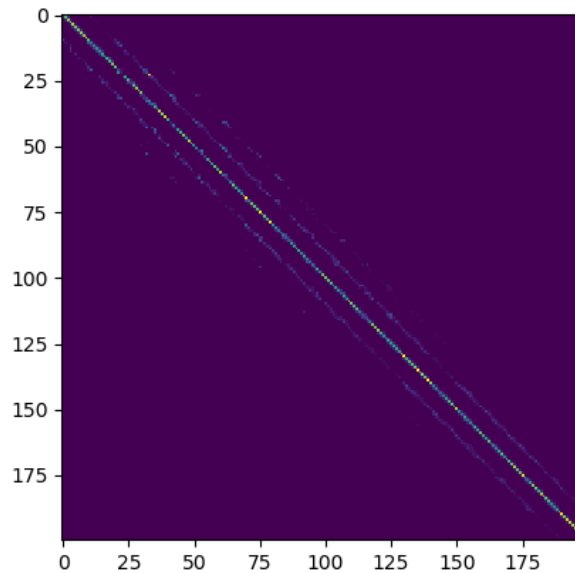


Figure 11: Transition matrix. Rows and columns are flattened histogram of a grid 20 cells high and 10 cells wide. Spatially adjacent grid cells are visible at a spacing of -11, -10, -9, 1, 10, and 11 cells from the diagonal. The intensity of pixels in the diagonal represents relative likelihood to stay in the same position.

245 Hidden Markov Models

246 Transition probabilities are most commonly modelled with Hidden Markov Models (HMM)
247 because of their ability to capture spatial and temporal dependencies. A recent introduction
248 to these methods is available provided by (Patterson et al., 2017). HMMs have successfully
249 been used to analyze movement of caribou (Franke et al., 2004), fruit flies (Holzmann et al.,
250 2006), and tuna (Patterson et al., 2018), among others. Trajectories are typically modelled
251 as bivariate time series consisting of step length and turn angle, regularly spaced in time.

252 Traja implements the rectangular spatial grid version of HMM with transitions.

253 The probability of transition from each cell to another cell is stored as a probability within the
254 transition matrix. This can be visualized as a heatmap and plotted with `plot_transition_ma`
255 `trix` (Figure 11).

256 Convex Hull

257 The convex hull of a subtrajectory is the set X of points in the Euclidean plane that is the
258 smallest convex set to include X . For computational efficiency, a geometric k-simplex can
259 be plotted covering the convex hull by converting to a Shapely object and using Shapely's
260 `convex_hull` method.

261 Recurrent Neural Networks

262 In recent years, deep learning has transformed the field of machine learning. For example,
263 the current state of the art models for a wide range of tasks, including computer vision,
264 speech to text, and pedestrian trajectory prediction, are achieved with deep neural networks.
265 Neural networks are essentially sequences of matrix operations and elementwise function ap-
266 plication based on a collection of computing units known as nodes or neurons. These units
267 perform operations, such as matrix multiplication on input features of a dataset, followed by
268 backpropagation of errors, to identify parameters useful for approximating a function.

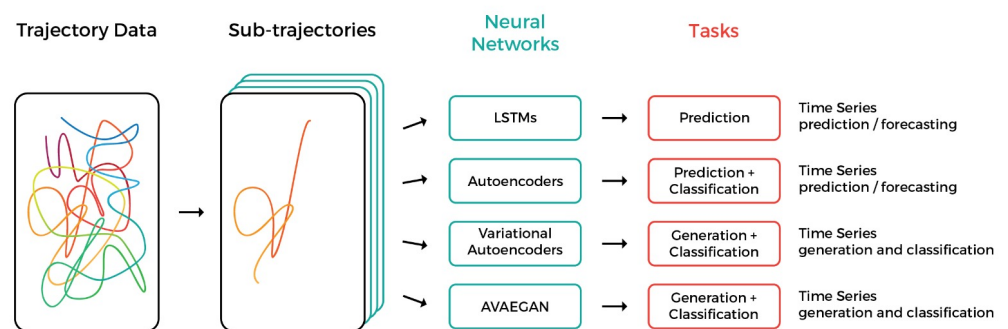


Figure 12: Neural network architectures available in Traja

269 Recurrent Neural Networks (RNNs) are a special type of Neural Networks that use a state
270 $S(t_{i-1})$ from the previous timestep t_{i-1} alongside $X(t_i)$ as input. They output a prediction
271 $Y(t_i)$ and a new state $S(t_i)$ at every step. Utilising previous states makes RNNs particularly
272 good at analyzing time series like trajectories, since they can process arbitrarily long inputs.
273 They remember information from previous time steps $X(t_{i-k}), \dots, X(t_{i-1})$ when processing
274 the current time step $X(t_i)$.

275 Trajectory prediction lets researchers forecast the location and trajectory of animals (Wijeyaku-
276 lasuriya et al., 2020). Where this technique works well, it is also a sign that the trajectory
277 is highly regular and, fundamentally, follows certain rules and patterns. When tracking an
278 animal live, it would also let researchers predict when it will arrive at a particular location, or
279 where it will go, letting them rig cameras and other equipment ahead of time.

280 A particularly interesting type of RNN is the Long Short Term Memory (LSTM) architecture.
281 Their layers use stacks of units, each with two hidden variables - one that quickly discards
282 old states and one that slowly does so - to consider relevant information from previous time
283 steps. They can thus look at a trajectory and determine a property of the animal - whether it
284 is sick or injured, say - something that is time-consuming and difficult to do by hand. They
285 can also predict future time steps based on past ones, letting researchers estimate where the
286 animal will go next. LSTMs can also classify trajectories, determining whether a trajectory
287 comes from an animal belonging in a specific category. This lets researchers determine how a
288 controlled or semi-controlled variable (e.g., pregnancy) changes the movement pattern of an
289 animal.

290 Traja implements neural networks by extending the widely used open source machine learning
291 library PyTorch (Paszke et al., 2019), primarily developed by Facebook AI Research Group.
292 Traja allows framework-agnostic modeling through data loaders designed for time series. In
293 addition, the Traja package comes with several predefined model architectures which can be
294 configured according to the user's requirements.

Because RNNs work with time series, the trajectories require special handling. The `traja.dataset.MultiModalDataLoader` efficiently groups subsequent samples and into series and splits these series into training and test data. It represents a Python iterable over the dataset and extends the PyTorch `DataLoader` class, with support for

- random, weighted sampling,
- data scaling,
- data shuffling,
- train/validation/test split.

`MultiModalDataLoader` accepts several important configuration parameters and allows batched sampling of the data. The two constructor arguments `n_past` and `n_future` specify the number of samples that the network will be shown and the number that the network will have to guess, respectively. `batch_size` is generally in the dozens and is used to regularise the network.

The RNNs also need to be trained - this is done by the high-level `Trainer` class below. It performs nonlinear optimisation with a Stochastic Gradient Descent-like algorithm. The `Trainer` class by default implements the Huber loss function (Huber, 1964), also known as smooth L_1 loss, which is a loss function commonly used in robust regression:

$$L_{\delta}(a) = \begin{cases} \frac{1}{2}a^2 & \text{for } |a| \leq \delta, \\ \delta(|a| - \frac{1}{2}\delta), & \text{otherwise.} \end{cases}$$

In comparison to mean-squared error loss, Huber loss is less sensitive to outliers in data: it is quadratic for small values of a , and linear for large values. It extends the PyTorch `SmoothL1Loss` class, where the d parameter is set to 1.⁶ A common optimization algorithm is ADAM and is Traja's default, but several others are provided as well. Although training with only a CPU is possible, a GPU can provide a 40 – 100 x speedup (Arpteg et al., 2018).

Recurrent Autoencoder Networks

Traja can also train autoencoders to either predict the future position of a track or classify the track into a number of categories. Autoencoders embed the time series into a time-invariant latent space, allowing representation of each trajectory or sub-trajectory as a vector. A class of well-separated trajectories would then be restricted to a region of the latent space. The technique is similar to Word2vec (Mikolov et al., 2013), where words are converted to a 100+ dimensional vector. In this approach, forecasting and classification are both preceded by training the data in an autoencoder, which learns an efficient representation of the data for further computation of the target function.

Traja allows training a classifier that works directly on the latent space output - since each class of trajectories converges to a distinct region in the latent space, this technique is often superior to classifying the trajectory itself. Traja trains classifiers for both Autoencoder-style and Variational Autoencoder-style RNNs. When investigating whether animal behavior has changed, or whether two experimental categories of animals behave differently, this unstructured data mining can suggest fruitful avenues for investigation.

References

- Amirian, J., Hayet, J.-B., & Pettre, J. (2019). Social Ways: Learning Multi-Modal Distributions of Pedestrian Trajectories with GANs. *arXiv:1904.09507 [cs]*. <https://doi.org/10.21105/joss.00118>

⁶<https://pytorch.org/docs/stable/generated/torch.nn.SmoothL1Loss.html>

1109/cvprw.2019.00359

- Arpteg, A., Brinne, B., Crnkovic-Friis, L., & Bosch, J. (2018). Software engineering challenges of deep learning. *2018 44th Euromicro Conference on Software Engineering and Advanced Applications (SEAA)*, 50–59. <https://doi.org/10.1109/seaa.2018.00018>
- Ayers, C., Armsworth, P., & Brosi, B. (2015). Determinism as a statistical metric for ecologically important recurrent behaviors with trapline foraging as a case study. *Behavioral Ecology and Sociobiology*, 69. <https://doi.org/10.1007/s00265-015-1948-3>
- Bak, P., Mansmann, F., Janetzko, H., & Keim, D. (2009). Spatiotemporal analysis of sensor logs using growth ring maps. *IEEE Transactions on Visualization and Computer Graphics*, 15, 913–920. <https://doi.org/10.1109/TVCG.2009.182>
- Bishop, C. (2006). *Pattern Recognition and Machine Learning*. Springer-Verlag. ISBN: 978-0-387-31073-2
- Bosch, J., Olsson, H. H., & Crnkovic, I. (2021). Engineering AI Systems: A Research Agenda [Chapter]. In *Artificial Intelligence Paradigms for Smart Cyber-Physical Systems*. <https://doi.org/10.4018/978-1-7998-5101-1.ch001>
- Calenge, C. (2006). The package adehabitat for the r software: Tool for the analysis of space and habitat use by animals. *Ecological Modelling*, 197, 1035.
- Chandra, R., Bhattacharya, U., Bera, A., & Manocha, D. (2019). TraPHic: Trajectory Prediction in Dense and Heterogeneous Traffic Using Weighted Interactions. *arXiv:1812.04767 [cs]*. <https://doi.org/10.1109/cvpr.2019.00868>
- Cox, G. E., Kachergis, G., & Shiffrin, R. M. (2012). *Gaussian Process Regression for Trajectory Analysis*. 6.
- Franke, A., Caelli, T., & Hudson, R. J. (2004). Analysis of movements and behavior of caribou (*Rangifer tarandus*) using hidden Markov models. *Ecological Modelling*, 173(2), 259–270. <https://doi.org/10.1016/j.ecolmodel.2003.06.004>
- Gillies, S., & others. (2007–). *Shapely: Manipulation and analysis of geometric objects*. toblerity.org. <https://github.com/Toblerity/Shapely>
- Gillies, S., & others. (2007–). *Shapely: Manipulation and analysis of geometric objects*. toblerity.org. <https://github.com/Toblerity/Shapely>
- Graser, A. (2019). MovingPandas: Efficient Structures for Movement Data in Python. *GI_Forum 2019, Volume 7*, 54–68. https://doi.org/10.1553/giscience2019_01_s54
- Grus, J. (2015). *Data Science from Scratch: First Principles with Python*. O'Reilly. ISBN: 978-1-4919-0142-7
- Harris, C. R., Millman, K. J., Walt, S. J. van der, Gommers, R., Virtanen, P., Cournapeau, D., Wieser, E., Taylor, J., Berg, S., Smith, N. J., Kern, R., Picus, M., Hoyer, S., Kerkwijk, M. H. van, Brett, M., Haldane, A., R'io, J. F. del, Wiebe, M., Peterson, P., ... Oliphant, T. E. (2020). Array programming with NumPy. *Nature*, 585(7825), 357–362. <https://doi.org/10.1038/s41586-020-2649-2>
- Holzmann, H., Munk, A., Suster, M., & Zucchini, W. (2006). Hidden Markov models for circular and linear-circular time series. *Environmental and Ecological Statistics*, 13(3), 325–347. <https://doi.org/10.1007/s10651-006-0015-7>
- Hsu, A. I., & Yttri, E. A. (2020). B-SOiD: An open source unsupervised algorithm for discovery of spontaneous behaviors. *bioRxiv*. <https://doi.org/10.1101/770271>
- Huang, K., Han, Y., Chen, K., Pan, H., Yi, W., Li, X., Liu, S., Wei, P., & Wang, L. (2020). Mapping Mouse Behavior with an Unsupervised Spatio-temporal Sequence Decomposition Framework. *bioRxiv*. <https://doi.org/10.1101/2020.09.14.295808>

- 381 Huber, P. J. (1964). Robust Estimation of a Location Parameter. *Annals of Mathematical*
382 *Statistics*, 35(1), 73–101. <https://doi.org/10.1214/aoms/1177703732>
- 383 Huette, S., Kello, C., Rhodes, T., & Spivey, M. (2013). Drawing from Memory: Hand-Eye
384 Coordination at Multiple Scales. *PloS One*, 8, e58464. <https://doi.org/10.1371/journal.pone.0058464>
- 386 Hunter, J. D. (2007). Matplotlib: A 2D graphics environment. *Computing in Science &*
387 *Engineering*, 9(3), 90–95. <https://doi.org/10.1109/MCSE.2007.55>
- 388 Jeung, H., Shen, H. T., & Zhou, X. (2007). Mining Trajectory Patterns Using Hidden Markov
389 Models. In I. Y. Song, J. Eder, & T. M. Nguyen (Eds.), *Data Warehousing and Knowledge*
390 *Discovery* (Vol. 4654, pp. 470–480). Springer Berlin Heidelberg. https://doi.org/10.1007/978-3-540-74553-2_44
- 392 Kareiva, P. M., & Shigesada, N. (1983). Analyzing insect movement as a correlated random
393 walk. *Oecologia*, 56(2-3), 234–238. <https://doi.org/10.1007/BF00379695>
- 394 Kerster, B. E., Rhodes, T., & Kello, C. T. (2016). Spatial memory in foraging games.
395 *Cognition*, 148, 85–96. <https://doi.org/10.1016/j.cognition.2015.12.015>
- 396 Liang, J., Jiang, L., Niebles, J. C., Hauptmann, A., & Fei-Fei, L. (2019). Peeking into the
397 Future: Predicting Future Person Activities and Locations in Videos. *arXiv:1902.03748*
398 *[cs]*. <https://doi.org/10.1109/cvprw.2019.00358>
- 399 Mathis, A., Mamidanna, P., Cury, K. M., Abe, T., Murthy, V. N., Mathis, M. W., & Bethge,
400 M. (2018). DeepLabCut: Markerless pose estimation of user-defined body parts with deep
401 learning. *Nature Neuroscience*. <https://doi.org/10.1038/s41593-018-0209-y>
- 402 McKinney, Wes. (2010). Data Structures for Statistical Computing in Python. In Stéfan van
403 der Walt & Jarrod Millman (Eds.), *Proceedings of the 9th Python in Science Conference*
404 (pp. 56–61). <https://doi.org/10.25080/Majora-92bf1922-00a>
- 405 McLean, D. J., & Volponi, M. A. S. (2018). Trajr: An R package for characterisation of
406 animal trajectories. *Ethology*, 124(6), 440–448. <https://doi.org/10.1111/eth.12739>
- 407 Mikolov, T., Sutskever, I., Chen, K., Corrado, G., & Dean, J. (2013). *Distributed representa-*
408 *tions of words and phrases and their compositionality*. <http://arxiv.org/abs/1310.4546>
- 409 Morato, R. G., Thompson, J. J., Paviolo, A., Torre, J. A. de L., Lima, F., McBride, R.
410 T., Paula, R. C., Cullen, L., Silveira, L., Kantek, D. L. Z., Ramalho, E. E., Maranhão,
411 L., Haberkfeld, M., Sana, D. A., Medellín, R. A., Carrillo, E., Montalvo, V., Monroy-
412 Vilchis, O., Cruz, P., ... Ribeiro, M. C. (2018). Jaguar movement database: A GPS-based
413 movement dataset of an apex predator in the Neotropics. *Ecology*, 99(7), 1691–1691.
414 <https://doi.org/10.1002/ecy.2379>
- 415 Neves, F. M., Viana, R. L., & Pie, M. R. (2017). Recurrence analysis of ant activity patterns.
416 *PLOS ONE*, 12(10), 1–15. <https://doi.org/10.1371/journal.pone.0185968>
- 417 Noonan, M. J., Fleming, C. H., Akre, T. S., Drescher-Lehman, J., Gurarie, E., Harrison, A.-L.,
418 Kays, R., & Calabrese, J. M. (2019). Scale-insensitive estimation of speed and distance
419 traveled from animal tracking data. *Movement Ecology*, 7(1), 35. <https://doi.org/10.1186/s40462-019-0177-1>
- 421 Paszke, A., Gross, S., Massa, F., Lerer, A., Bradbury, J., Chanan, G., Killeen, T., Lin, Z.,
422 Gimelshein, N., Antiga, L., Desmaison, A., Kopf, A., Yang, E., DeVito, Z., Raison, M.,
423 Tejani, A., Chilamkurthy, S., Steiner, B., Fang, L., ... Chintala, S. (2019). PyTorch: An
424 imperative style, high-performance deep learning library. In H. Wallach, H. Larochelle, A.
425 Beygelzimer, F. dAlché-Buc, E. Fox, & R. Garnett (Eds.), *Advances in neural information*
426 *processing systems* 32 (pp. 8024–8035). Curran Associates, Inc. [http://papers.neurips.](http://papers.neurips.cc/paper/9015-pytorch-an-imperative-style-high-performance-deep-learning-library.pdf)
427 [cc/paper/9015-pytorch-an-imperative-style-high-performance-deep-learning-library.pdf](http://papers.neurips.cc/paper/9015-pytorch-an-imperative-style-high-performance-deep-learning-library.pdf)

- 428 Patterson, T. A., Eveson, J. P., Hartog, J. R., Evans, K., Cooper, S., Lansdell, M., Hobday,
429 A. J., & Davies, C. R. (2018). Migration dynamics of juvenile southern bluefin tuna.
430 *Scientific Reports*, 8(1), 1–10. <https://doi.org/10.1038/s41598-018-32949-3>
- 431 Patterson, T. A., Eveson, J. P., Hartog, J. R., Evans, K., Cooper, S., Lansdell, M., Hobday,
432 A. J., & Davies, C. R. (2018). Migration dynamics of juvenile southern bluefin tuna.
433 *Scientific Reports*, 8(1), 1–10. <https://doi.org/10.1038/s41598-018-32949-3>
- 434 Patterson, T. A., Parton, A., Langrock, R., Blackwell, P. G., Thomas, L., & King, R. (2017).
435 Statistical modelling of individual animal movement: An overview of key methods and a
436 discussion of practical challenges. *ASTA Advances in Statistical Analysis*, 101(4), 399–438.
437 <https://doi.org/10.1007/s10182-017-0302-7>
- 438 Patterson, T. A., Parton, A., Langrock, R., Blackwell, P. G., Thomas, L., & King, R. (2017).
439 Statistical modelling of individual animal movement: An overview of key methods and a
440 discussion of practical challenges. *ASTA Advances in Statistical Analysis*, 101(4), 399–438.
441 <https://doi.org/10.1007/s10182-017-0302-7>
- 442 Rasmussen, CE., & Williams, CKI. (2006). *Gaussian Processes for Machine Learning*. Biolo-
443 gische Kybernetik.
- 444 Ross, J. M., Warlaumont, A. S., Abney, D. H., Rigoli, L. M., & Balasubramaniam, R. (2016).
445 Influence of musical groove on postural sway. *Journal of Experimental Psychology: Human*
446 *Perception and Performance*, 42(3), 308–319. <https://doi.org/10.1037/xhp0000198>
- 447 Rowcliffe, J. M., Carbone, C., Kays, R., Kranstauber, B., & Jansen, P. A. (2012). Bias in
448 estimating animal travel distance: The effect of sampling frequency. *Methods in Ecology*
449 *and Evolution*, 3(4), 653–662. <https://doi.org/10.1111/j.2041-210X.2012.00197.x>
- 450 Savitzky, Abraham., & Golay, M. J. E. (1964). Smoothing and Differentiation of Data by
451 Simplified Least Squares Procedures. *Analytical Chemistry*, 36(8), 1627–1639. <https://doi.org/10.1021/ac60214a047>
- 452 <https://doi.org/10.1021/ac60214a047>
- 453 sgoldenlab, Choong, J. J., Nilsson, S., Islam, A., & sophihwang26. (2021). *Sgoldenlab/simba:*
454 *SimBA: Release v1.3* (Version v1.3) [Computer software]. Zenodo. [https://doi.org/10.](https://doi.org/10.5281/zenodo.4521178)
455 [5281/zenodo.4521178](https://doi.org/10.5281/zenodo.4521178)
- 456 Shenk, J., Lohkamp, K. J., Wiesmann, M., & Kiliaan, A. J. (2020). Automated Analysis of
457 Stroke Mouse Trajectory Data With Traja. *Frontiers in Neuroscience*, 14. [https://doi.](https://doi.org/10.3389/fnins.2020.00518)
458 [org/10.3389/fnins.2020.00518](https://doi.org/10.3389/fnins.2020.00518)
- 459 Shockley, K., Santana, M.-V., & Fowler, C. (2003). Mutual interpersonal postural constraints
460 are involved in cooperative conversation. *Journal of Experimental Psychology. Human*
461 *Perception and Performance*, 29, 326–332. <https://doi.org/10.1037/0096-1523.29.2.326>
- 462 Solla, S. R. D., Bonduriansky, R., & Brooks, R. J. (1999). Eliminating autocorrelation reduces
463 biological relevance of home range estimates. *Journal of Animal Ecology*, 68(2), 221–234.
464 <https://doi.org/10.1046/j.1365-2656.1999.00279.x>
- 465 Spink, A. J., Tegelenbosch, R. A. J., Buma, M. O. S., & Noldus, L. P. J. J. (2001). The Etho-
466 Vision video tracking system—A tool for behavioral phenotyping of transgenic mice. *Phys-*
467 *iology & Behavior*, 73(5), 731–744. [https://doi.org/10.1016/S0031-9384\(01\)00530-3](https://doi.org/10.1016/S0031-9384(01)00530-3)
- 468 Sridhar, V. H. (2017). *Vivekhsridhar/tracktor: tracktor* (tracktor) [Computer software]. Zen-
469 odo. <https://doi.org/10.5281/zenodo.1134016>
- 470 team, T. pandas development. (2020). *Pandas-dev/pandas: pandas* (latest) [Computer
471 software]. Zenodo. <https://doi.org/10.5281/zenodo.3509134>
- 472 Van Galen, G. P., Van Doorn, R. R., & Schomaker, L. R. (1990). Effects of motor pro-
473 gramming on the power spectral density function of finger and wrist movements. *Jour-*
474 *nal of Experimental Psychology: Human Perception and Performance*, 16(4), 755–765.
475 <https://doi.org/10.1037/0096-1523.16.4.755>

- 476 Wang, X. (2017). *Modeling Trajectory as Image: Convolutional Neural Networks*
477 *for Multi-scale Taxi Trajectory Prediction*. [https://www.academia.edu/34767293/](https://www.academia.edu/34767293/Modeling_Trajectory_as_Image_Convolutional_Neural_Networks_for_Multi-scale_Taxi_Trajectory_Prediction)
478 [Modeling_Trajectory_as_Image_Convolutional_Neural_Networks_for_Multi-scale_](https://www.academia.edu/34767293/Modeling_Trajectory_as_Image_Convolutional_Neural_Networks_for_Multi-scale_Taxi_Trajectory_Prediction)
479 [Taxi_Trajectory_Prediction](https://www.academia.edu/34767293/Modeling_Trajectory_as_Image_Convolutional_Neural_Networks_for_Multi-scale_Taxi_Trajectory_Prediction)
- 480 Waskom, M. L. (2021). Seaborn: Statistical data visualization. *Journal of Open Source*
481 *Software*, 6(60), 3021. <https://doi.org/10.21105/joss.03021>
- 482 Wijeyakulasuriya, D. A., Eisenhauer, E. W., Shaby, B. A., & Hanks, E. M. (2020). Machine
483 learning for modeling animal movement. *PLOS ONE*, 15(7), 1–30. [https://doi.org/10.](https://doi.org/10.1371/journal.pone.0235750)
484 [1371/journal.pone.0235750](https://doi.org/10.1371/journal.pone.0235750)
- 485 Zheng, Y. (2015). Trajectory Data Mining: An Overview. *ACM Transaction on Intelli-*
486 *gent Systems and Technology*. [https://www.microsoft.com/en-us/research/publication/](https://www.microsoft.com/en-us/research/publication/trajectory-data-mining-an-overview/)
487 [trajectory-data-mining-an-overview/](https://www.microsoft.com/en-us/research/publication/trajectory-data-mining-an-overview/)

DRAFT